

## **Focal Plane Detector System of SHARAQ Spectrometer**

S. Michimasa, H. Tokieda, S. Noji, S. Ota, S. Shimoura, T. Uesaka, H. Sakai,  
P. Roussel-Chomaz, J.F. Libin, P. Gangnant, et al.

► **To cite this version:**

S. Michimasa, H. Tokieda, S. Noji, S. Ota, S. Shimoura, et al.. Focal Plane Detector System of SHARAQ Spectrometer. RIKEN Accelerator Progress Report, 2010, 43, pp.174-175. in2p3-00553112

**HAL Id: in2p3-00553112**

**<http://hal.in2p3.fr/in2p3-00553112>**

Submitted on 6 Jan 2011

**HAL** is a multi-disciplinary open access archive for the deposit and dissemination of scientific research documents, whether they are published or not. The documents may come from teaching and research institutions in France or abroad, or from public or private research centers.

L'archive ouverte pluridisciplinaire **HAL**, est destinée au dépôt et à la diffusion de documents scientifiques de niveau recherche, publiés ou non, émanant des établissements d'enseignement et de recherche français ou étrangers, des laboratoires publics ou privés.

## Focal Plane Detector System of SHARAQ Spectrometer

S. Michimasa,<sup>1</sup> H. Tokieda,<sup>1</sup> S. Noji,<sup>2</sup> S. Ota,<sup>1</sup> S. Shimoura,<sup>1</sup> T. Uesaka,<sup>1</sup> H. Sakai,<sup>2</sup>  
P. Roussel-Chomaz,<sup>3</sup> J-F. Libin,<sup>3</sup> P. Gangnant,<sup>3</sup> and C. Spitaels<sup>3</sup>

[SHARAQ spectrometer, cathode-readout drift chamber]

The construction of the SHARAQ spectrometer<sup>1)</sup> and the high-resolution beam line<sup>2)</sup> was completed at the RI Beam Factory (RIBF) at RIKEN in March 2009, and commissioning beam runs were performed in March and May 2009. During the beam runs, we examined dispersion-matching ion optics and evaluated the performance of the detectors installed in the focal planes of the beam line and that of the spectrometer. Valuable information on the basic performance of the high-resolution spectrometer system was obtained. This report describes the basic performance of the detector system installed in the final momentum-dispersive focal plane of the SHARAQ spectrometer.

Figure 1 shows the detector setup used in the commissioning runs. Two tracking detectors and two plastic scintillators were installed in the final focal plane of the SHARAQ spectrometer. The focal plane is located

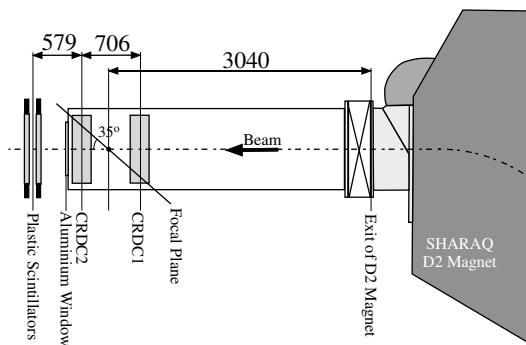


Fig. 1. Detector setup in the final focal plane of SHARAQ in the commissioning runs (top view). The detector system consists of two tracking detectors and two plastic scintillators.

3.04 m downstream from the exit of the SHARAQ D2 magnet and inclined at 35 degrees relative to the central orbit. The beam particles passed through the tracking detectors installed in vacuum and then passed into the air through a 10 mm-thick aluminum window. The plastic scintillators were placed downstream of the aluminum window.

The plastic scintillators were used to measure the timings of beam particles at the focal plane and to measure the energy deposits in them. The two-layer configuration of the scintillators was effective in rejecting cosmic-ray events. The measured results ob-

tained from each scintillator were read out by two photomultiplier tubes attached to the left and right of the scintillators. The size of the plastic scintillator was  $1110 \text{ (H)} \times 300 \text{ (V)} \times 5 \text{ (T)} \text{ mm}^3$ . Charge and timing data obtained from the scintillators were collected using charge-to-time converters (QTCs)<sup>3)</sup> and multi-hit TDCs. We were able to identify  $^{12}\text{N}$  and  $^{11}\text{C}$  particles with a separation of more than  $5 \sigma$ .

The tracking of particles were performed using two cathode-readout drift chambers (CRDCs)<sup>4,5)</sup>. The CRDCs have manufactured in January 2009 in collaboration with the detector developing group of GANIL. The structure of the CRDC is described in detail in Ref.<sup>5)</sup>. In the commissioning runs, the CRDCs were operated with isobutane gas at 15 or 30 torr for the detection of various light nuclei such as  $t$ ,  $^6\text{He}$ ,  $^9\text{Li}$ ,  $^{12}\text{B}$ , and  $^{12,14}\text{N}$  at around 200A–250A MeV.

The CRDC transmits two signals from the anode wires and two multiplexed signals from the cathode pads. The anode signals were used to deduce the drift time and the charge of secondary electrons. The preamplifiers for the anodes were charge sensitive; they had a gain of 0.9 V/pC and a time constant of 20 ns. The time reference for the measurement of the drift time was provided by the plastic scintillators. Since the anode signal is generated when an avalanche occurs around the anode wires, the drift times are determined by the difference between the anode timing signal and the timing signal of the plastic scintillator. We operated CRDCs with drift electric fields of 83.3 (140) V/cm using 15-(30-)torr isobutane. The drift velocity of the secondary electrons were 5.9 cm/μs at 15 torr and 5.3 cm/μs at 30 torr, respectively. These values are approximately equal to those evaluated by using the GARFIELD code<sup>6)</sup>. Under the above mentioned conditions, the vertical position resolution was approximately 0.9 mm (FWHM), which is inferior to the design value by a factor of 2. We are continuing data analysis in order to improve the position resolution.

Figure 2 shows the avalanche gain measured by CRDCs operated with 30-torr isobutane as a function of the voltage supplied to the anode wires. CRDC1 (CRDC2) corresponds to the upstream (downstream) tracking chamber in Fig. 1. The avalanche gain of CRDC2 was consistently smaller than that of CRDC1. This difference in the gains is considered to be due to the difference in their configurations. In CRDC1, potential wires are placed between anode wires, while CRDC2 has no potential wires; this has been schemati-

<sup>1</sup> Center for Nuclear Study, University of Tokyo

<sup>2</sup> Department of Physics, University of Tokyo

<sup>3</sup> GANIL, France

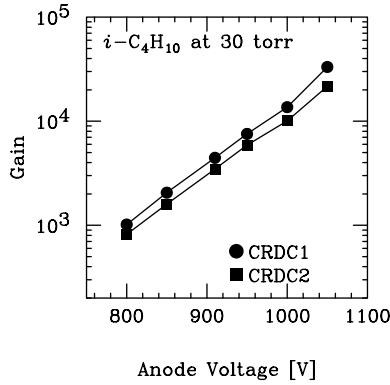


Fig. 2. Avalanche gain of CRDCs measured using isobutane gas at 30 torr. The definitions of CRDC1 and CRDC2 are described in the text.

cally depicted in Fig. 2 of Ref.<sup>5</sup>). However, we demonstrated that both the CRDCs achieved an avalanche gain higher than the required gain of  $10^4$ .

The detection efficiency of the CRDC is defined here as the ratio of the detection using the anode signal to the detection by the plastic scintillators. Figure 3 shows the detection efficiency of CRDC1 as a function of the supplied anode voltage. Fig. 3(a) shows the detection efficiency curves for  $^{14}\text{N}$  ions at 250A MeV in the 15- and 30-torr operations, and Fig. 3(b) shows the detector efficiency for lighter particles at around 220A MeV in the 30-torr operation. It was confirmed

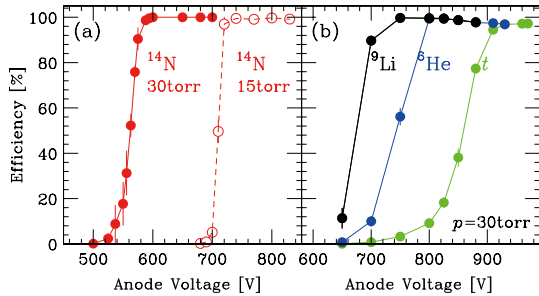


Fig. 3. (a) Detection efficiency for 250A-MeV  $^{14}\text{N}$  ions with the 15- and 30-torr operations. (b) Detection efficiency for  $t$ ,  $^6\text{He}$ ,  $^9\text{Li}$  particles with the 15- and 30-torr operations.

that the CRDCs designed for SHARAQ will achieve detection efficiencies of approximately 100% for 200A-MeV tritons even when operated using 30-torr isobutane gas.

The horizontal position in the focal plane is determined by the charge distribution on the cathode pads. The charge signals from the cathode pads were read out by using GASSIPLEX chips<sup>7</sup>) and a CRAMS module<sup>8</sup>). The pedestals of the channels the GASSIPLEX chip ranged from 60 to 70 mV and were stable ( $< 2$  mV) over the 10-day measurements. The track-and-hold signals were generated by the timing of the anode signal of the CRDC under the condition that two plastic scintillators and the anode were detected

simultaneously. In the commissioning run, we applied anode voltages that were 30 V higher than the voltages for which the detection efficiencies were 100%. At the supplied voltage, induced charges were distributed over approximately 10 cathode pads, and the maximum induced charge was present around the middle of the dynamic range of GASSIPLEX. The horizontal position was deduced by fittings of the charge distributions to a function

$$q(x) = a_1 \cdot \text{sech}^2 [\pi(x - a_2)/a_3],$$

where  $a_i$  ( $i = 1, 2, 3$ ) are fitting parameters<sup>9</sup>). The horizontal position corresponds to  $a_2$ . The typical resolutions of horizontal position were estimated to be 500  $\mu\text{m}$  and 700  $\mu\text{m}$  (FWHM) for  $^{14}\text{N}$  at 250A-MeV and  $^6\text{He}$  at 220A-MeV, respectively.

In summary, we examined the detector system installed in the focal plane of the SHARAQ spectrometer in the commissioning runs of the SHARAQ spectrometer by using light radioactive isotopes at 200A–250A MeV. All the detectors were operated successfully and the basic data on their performance were obtained. Identification of particles with atomic numbers  $Z$  of around 7 was performed by using plastic scintillators. Under the present conditions, the position resolution of CRDCs was estimated to be 0.9 mm (FWHM) in the horizontal direction and 0.7 mm (FWHM) in the vertical direction. In the first experiment<sup>10</sup>) that was performed in November 2009, the focal plane detector system was used, and the data on the ( $t, ^3\text{He}$ ) reactions at 300A MeV were obtained. Further analysis is now in progress in order to optimize the detectors' parameters and to improve the data-analysis algorithm used in the detectors.

## References

- 1) T. Uesaka et al.: Nucl. Instrum. Methods Phys. Res. B **266**, 4218 (2008).
- 2) T. Kawabata et al.: Nucl. Instrum. Methods Phys. Res. B **266**, 4201 (2008); Y. Yanagisawa et al.: Bull. Amer. Phys. Soc. **54**, 48 (2009).
- 3) H. Nishino et al.: Nucl. Instrum. Methods Phys. Res. A **610**, 710 (2009).
- 4) M.H. Tanaka et al.: Nucl. Instrum. Methods Phys. Res. A **362**, 521 (1995).
- 5) S. Michimasa et al.: CNS-REP-80, (2009) 55.
- 6) R. Veenhof, GARFIELD, CERN Program Library W5050.
- 7) The GASSIPLEX is a re-designed chip of the AMPLEX by J.C. Santiard of CERN. The AMPLEX is described in E. Beuville et al.: Nucl. Instrum. Methods Phys. Res. A **288**, 157 (1990).
- 8) V551 C.A.E.N sequencer User Guide, V550 C.A.E.N CRAMS User Guide.
- 9) K. Lau and J. Pyrlík: Nucl. Instrum. Methods Phys. Res. A **366**, 298 (1995).
- 10) K. Miki et al.: RIKEN Accel. Prog. Rep. **43**, (2010).